Journal of Fluorine Chemistry 213 (2018) 80–86

Contents lists available at ScienceDirect

Journal of Fluorine Chemistry

journal homepage: www.elsevier.com/locate/fluor

AlN coatings on Hastelloy-N alloy offering superior corrosion resistance in LiF-KF-NaF molten salt

Hongmei Zhu[a], Baichun Li[a], Minghui Chen[a], Zhili Liu[a], Zhongfeng Tang[b,*], Changjun Qiu[a,*]

[a] School of Mechanical Engineering, University of South China, Hengyang, Hunan 421001, China
[b] Shanghai Institute of Applied Physics, Chinese Academy of Sciences, Shanghai 201800, China

ARTICLE INFO

Keywords:
Hastelloy-N alloy
Laser cladding
AlN coating
Corrosion resistance
LiF-KF-NaF molten salt

ABSTRACT

High-temperature corrosion resistance is a big issue for structural materials in molten salt reactors. A simple but effective laser cladding technique has been utilized for producing a compact AlN coating on Hastelloy-N alloy. The results show that the laser-cladded AlN coating improves the compatibility of Hastelloy-N alloy in LiF-NaF-KF molten salt at 900 °C significantly. The uncoated Hastelloy-N alloy is composed of γ-Ni and M_6C phases, showing a typical intergranular corrosion with a precipitation of new $Cr_9Mo_{21}Ni_{20}$ phase after corrosion. In contrast, the AlN coating exhibits a silghtly unifrom corrosion and protects the Hastelloy-N substrate effectively. The laser-cladded specimes are composed of γ-Ni and AlN before and after corrosion. The possible reasons for the discrepancy in the corrosion behavior between uncoated and coated specimens are discussed in this job.

1. Introduction

Eutectic LiF-KF-NaF salt (46.5–11.5–42.0 mol %, FLiNaK) is representative of heating transfer fluids in molten salt reactors (MSR), with superior high-temperature stability and high heat flux. However, it is highly corrosive to materials that are used in the high-temperature environments [1]. Hastelloy-N alloy has been considered one of the most appropriate structural materials in FLiNaK molten salt. However, it remains a big challenge for applications above 700 °C due to the inherent thermodynamic instability of protective surface oxide layers [2–4].

Up to now, there are limited reports on surface protective coatings for structural materials in the corrosive molten fluoride salt [5–7], including pure Ni coating on Incoloy-800 by electroplating [5], pure Ni coating on Inconel 617 by laser cladding and chemical vapor deposition [6], and Cr_3C_2 coating on Haynes-230 by spraying and carburization [7]. In comparison with electroplating and thermal spraying coating techniques, laser cladding possesses distinctively inherent merits such as high efficiency, highly refined microstructure, strong coating adhesion via metallurgical bonding and easily controlled coating thickness [8].

Aluminum nitride (AlN) is an ideal candidate attributed to its remarkable properties, including high hardness (> 11 GPa), high-temperature stability (> 2000 °C), excellent corrosion resistance in liquid metal and FLiNaK [9–11]. However, AlN coating has not been applied onto the structural materials to enhance its corrosion resistance in FLiNaK to our best knowledge. Therefore, we have fabricated, for the first time, an AlN coating on Hastelloy-N alloy by the laser cladding technique in this work, aiming at providing a potential strategy for a better performance of Hastelloy-N in molten fluoride salt.

2. Experimental

The material studied is Hastelloy-N alloy with a chemical composition as shown in Table 1. The Hastelloy-N was cut into strips of 60 mm × 60 mm × 5 mm dimension, followed by grinding down to a 1200 grit finish with SiC papers, sand blasting, and cleaning with acetone.

High-purity FLiNaK was received from Shanghai Institute of Applied Physics, Chinese Academy of Sciences. The salt sample was analyzed using inductively coupled plasma-optical emission spectrometer (ICP-OES) before detecting the following impurities: 11 ppm Ca, 10 ppm Ni, 7 ppm Mg, and 101 ppm Si. Other elements were determined below 5 ppm or below the quantitative detection limits of ICP-OES. The concentrations of residual oxygen and water in FLiNaK were 300 ppm and 100 ppm as determined through a LECO oxygen analyzer and Karl–Fischer titration, respectively.

Commercial AlN powders of 75 μm in diameter were used for laser cladding. A TJ-HL-T5000 5 kW CO_2 laser was used for laser cladding with the following parameters: laser power 2.6 kW, laser scanning

* Corresponding authors at: P.O. Box 800-204, Shanghai, 201800, China.
E-mail addresses: tangzhongfeng@sinap.ac.cn (Z. Tang), qiuchangjun@hotmail.com (C. Qiu).

https://doi.org/10.1016/j.jfluchem.2018.07.007
Received 25 May 2018; Received in revised form 17 July 2018; Accepted 19 July 2018
Available online 21 July 2018
0022-1139/

Table 1
The chemical compositions of Hastelloy-N alloy (wt.%).

Element	Ni	Cr	Mo	Fe	Mn	Al	W	Si	C
Mass fraction (%)	Bal.	7.01	16.80	4.16	0.52	0.28	0.20	0.36	0.06

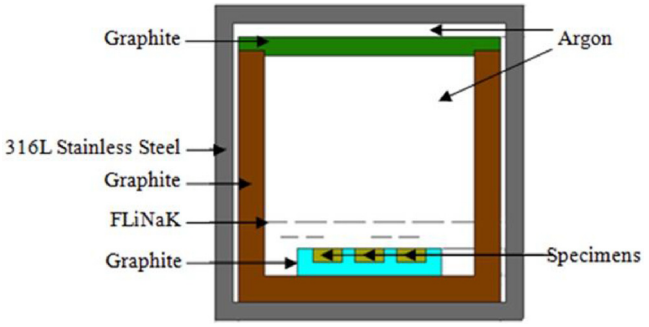

Fig. 1. Schematic of the experimental setup.

Table 2
Corrosion weight loss of Hastelloy-N alloy and the AlN coated specimen.

Specimens	Hastelloy-N alloy	AlN coated specimen
Corrosion weight loss rate (mg/mm^2)	0.3164 ± 0.0003	0.1039 ± 0.0002

speed 6 mm/s, laser beam size 4 mm, multi-tracking overlapping rate 50%, powder feeding rate 6.5 g/min and the Ar flow rate 40 L/min.

The corrosion experiment is schematically illustrated in Fig. 1. For the laser cladded specimens, only the coated surface was exposed to the molten salt. Meanwhile, a dry Ar gas stream was introduced to maintain an inert surface environment for the molten salts and to carry possible gaseous HF away from the furnace. After an exposure of 100 h at 900 °C, the furnace was then cooled down to room temperature. The specimens were retrieved from the solidified salt bed, then cleaned ultrasonically in 1.0 mol L^{-1} $Al(NO_3)_3$ solution, deionized water and ethanol in sequence.

Weight loss of the specimens was evaluated by weight change measurement using a high precision balance (accuracy ± 0.1 mg). Weight loss (R) was calculated by the following formula: $R = (|m_0 - m_1|)/S_0$ (1), where m_0 and m_1 are the mass of the specimen before and after corrosion, respectively, and S_0 is the corrosion area of the specimen [12].

Microstructural characterization of the specimens was carried out by scanning electron microscopy (SEM, ZEISS MERLIN Compact) equipped with an Oxford energy-dispersive X-ray spectrometry (EDS), X-ray diffraction (XRD, X-D6).

3. Results and discussion

The corrosion rate of the specimens was evaluated by weight change measurement. A careful calculation shown in Table 2 indicates that the weight loss of Hastelloy-N alloy and the AlN-coated specimen after a 100 h exposure in FLiNaK at 900 °C is 0.3164 ± 0.0003 mg/mm^2 and 0.1039 ± 0.0002 mg/mm^2, respectively. That is, the corrosion loss rate of the AlN-coated specimen is merely 1/3 of that of the pure Hastelloy-N alloy. Obviously, the laser cladded AlN-coating can significantly enhance the corrosion resistance of Hastelloy-N alloy in FLiNaK molten salt.

In order to examine the changes of phase constituents and elemental distribution of both the uncoated and coated specimens before and after corrosion tests, XRD and EDS line scanning were carried out in this experiment as seen in Fig. 2.

The uncoated Hastelloy-N alloy is a typical solid-solution strengthened alloy with the phase constitution of γ-Ni matrix and M_6C phase (M represents the metal elements such as Ni, Mo and Cr) [12–15], as shown in Fig. 2a. Such primary carbide M_6C is of crystal structure with an excellent high-temperature stability up to about 1250 °C [12–15]. After a 100 h exposure in FLiNaK molten salt at 900 °C, a newly-precipitated $Cr_9Mo_{21}Ni_{20}$ phase was identified according to International Centre for Diffraction Data (ICDD #07-0050). $Cr_9Mo_{21}Ni_{20}$ phase has been widely reported to P phase as an equilibrium structure in the Ni-Mo-Cr superalloys after a long-term isothermal heat treatment [16]. It is notable that the XRD peaks corresponding to γ-Ni phase slightly shift rightward after corrosion. This is probably caused by the lattice distortion due to some dissolved atoms at a high temperature, coinciding with the findings about Hastelloy-N alloy after a corrosion in FLiNaK molten salt at 850 °C for 400 h [7]. It is clearly seen from Fig. 2b that both pre- and post-corrosion coated specimens are mainly composed of AlN and γ-Ni phases, where the existence of γ-Ni phase is caused by elemental diffusion from of Hastelloy-N substrate during high-temperature laser cladding. Besides, a slight shift of γ-Ni peaks towards high angles can be also visible after corrosion. This is similar to the slightly right shift of γ-Ni peaks in Hastelloy-N alloy after a corrosion test as shown in Fig. 2b. As shown in Fig. 2c and d, the domain concentration change is invisible in the Hastelloy-N alloy and AlN-coated specimens before and after corrosion, completely different from the obvious concentration gradient change of element Cr in Hastelloy-N alloy after corrosion in FLiNaK [3,17,18]. The elementary composition of Hastelloy-N alloy and AlN-coated specimens have not been changed before and after corrosion. In addition, some peaks in the EDS line scanning of element Al and Mo correspond to AlN and Mo-rich phase, respectively. From Fig. 2, it is evidence that AlN coating is of high stability and resistance to chemical attacks in the high-temperature molten fluoride salt.

Fig. 3a and b show the surface SEM images of the uncoated Hastelloy-N alloy before and after corrosion, respectively. Meanwhile, Fig. 3c and d show the cross-section SEM images of the uncoated Hastelloy-N alloy before and after corrosion, respectively. The original Hastelloy-N alloy is of homogeneous microstructure with grain size of 50 ~ 100 μm and grey M_6C particles are dispersed in the matrix (Fig. 3a and c). After corrosion test, a severe intergranular corrosion is observed in Fig. 3b and d, consistent with other reports regarding the element Cr in Hastelloy-N alloy reacting and dissolving in the molten salt initially to produce a Cr-depleted surface layer [3,17,18]. The high-energy grain boundaries may become a rapid diffusion channel for element Cr, and consequently result in severe intergranular corrosion of Hastelloy-N alloy. The observed voids along the grain boundary is mainly attributed to the aggregation of vacancies left by the outward diffusion of Cr [4,7,8,19].

In addition, it is clearly visible from a high-magnification image in Fig. 3e that a large amount of secondary particles were precipitated in Hastelloy-N alloy after corrosion. As revealed by the EDS microanalysis results in Table 3, the grey particle '2' with a larger size (2 ~ 5 μm) is of similar composition with the gray particle '1' in the as-received Hastelloy-N alloy, these particles can be determined as M_6C. Besides, the smaller white particle '3' in size of ~ 500 nm having a Cr/Mo/Ni atomic ratio of 14:35:33 stoichiometry, can be reasonably considered as $Cr_9Mo_{21}Ni_{20}$ phase in good agreement with XRD analysis.

Fig. 4 shows the top-view SEM images and EDS results of the AlN-coated specimens before and after corrosion. As seen from Fig. 4a and c, a compact and extremely fine-grained AlN coating has been prepared by the laser cladding process. After experiencing a 100 h corrosion at 900 °C in FLiNaK, the AlN coating layer exhibits slightly homogeneous corrosion as shown in Fig. 4b and d. It can be discernible from Fig. 4c and d that there are mainly two different types of particles dispersed in the pre- and post-corrosion coating layer, i.e., one is the black granular particles marked as '1' by black arrows and the other is the grey irregular particles marked as '2' by white arrows. The EDS result for particle '1' and particle '2' is shown in Fig. 4e and f, respectively. In